

A High-Performance Strain Sensing Microsystem with Remote RF Power Capability

Darrin J. Young and Wen H. Ko

EECS Department, Case Western Reserve University, Cleveland, Ohio, USA, 44106

Abstract

This paper describes a high-performance strain sensing microsystem with a remote RF powering capability. A MEMS capacitive strain sensor converts an input strain to a capacitance change with a sensitivity of 26.5 aF per 0.1 $\mu\epsilon$. Low-noise integrated sensing electronics employing a continuous time synchronous detection architecture convert the capacitive signal to an output voltage for further signal processing. An RF to DC converter based on inductive coupled coils converts a 50 MHz AC signal to a stable DC supply of 2.8 V with a current driving capability of 2 mA, sufficient to power the interface sensing electronics. The prototype microsystem achieves a minimum detectable strain of 0.09 $\mu\epsilon$ over a 10 kHz bandwidth with a dynamic range of 81 dB. The sensing electronics consume 1.5 mA from a 2.8 V supply.

Introduction

High-performance strain sensing microsystem consisting of sensors and interface electronics are highly critical for advanced industrial applications, such as point-stress and torque sensing for ball-bearings, rotating shafts and blades, etc. The information is important for optimizing system performance, understanding material fatigue, and achieving a reliable system monitoring and intelligent control. Stringent performance requirements with a high sensitivity of 0.1 $\mu\epsilon$ over a wide bandwidth of 10 kHz and a large dynamic range of 80 dB are demanded for these applications. Conventional strain sensors made of metal foils and semiconductor piezoresistive elements suffer from a limited sensitivity, large temperature dependence, turn-on drift, and poor time stability, thus inadequate for high-performance and low cost applications [1, 2].

MEMS resonant strain sensors [3] have been demonstrated to achieve a high performance by converting an input strain to a change in the device resonant frequency, but requires a large operating voltage of approximately 100 V, thus undesirable for low voltage and low power integrated systems. MEMS capacitive strain sensors, however, are attractive due to a number of key advantages such as high sensitivity, minimum temperature dependence and turn-on drift, low noise, large dynamic range, and potential monolithic integration with low power

CMOS electronics [4, 5], and thus will be employed for the prototype system design.

Industrial strain sensing applications further impose significant design challenges due to various rotating mechanical components employed in the system. Therefore, complete stand-alone microsystems with remote powering and data telemetry capabilities are highly desirable. Inductive-coupling-based powering techniques have been widely used for biomedical implant applications [6-8], where coupling coils are fixed at certain positions. This project aims to develop a remote powering technique, which can achieve an useful coupling distance and is insensitive to mechanical rotations for advanced industrial sensing applications.

In this paper, low-noise CMOS integrated sensing electronics interfaced with a capacitive MEMS strain sensor and powered by a stable remote RF powering system are presented to achieve a sensing dynamic range of 81 dB with a strain resolution of 0.09 $\mu\epsilon$ over a 10 KHz bandwidth, corresponding to an equivalent displacement resolution of $0.009 \text{ \AA}/\sqrt{Hz}$, which is twice better than that of state-of-the-art MEMS inertial sensors [9, 10]. The demonstrated performance also represents two orders of magnitude improvement compared to any existing commercial strain sensing technologies.

Microsystem Architecture

Figure 1 presents a proposed stand-alone microsystem architecture, which consists of a MEMS capacitive strain sensor and interface electronics with coil loops for remote powering and data telemetry. The microsystem is attached to the surface of a rotating iron shaft with a diameter of 3 inches for the prototype design. An internal coil is wound around the shaft and separated from the external coil by one inch. This configuration is critical for achieving a stable and uniform coil coupling during shaft rotation. The rotating of the shaft produces a rotational torque, thus a surface strain, which can be sensed by the MEMS strain sensor. The sensor output is then converted to a voltage, followed by digitization and data telemetry to a nearby receiver for signal acquisition and analysis. This paper focuses on the design and performance characterization of a MEMS strain sensor, low noise interface electronics, and a remote RF powering system. The sensor data telemetry system is currently under development.

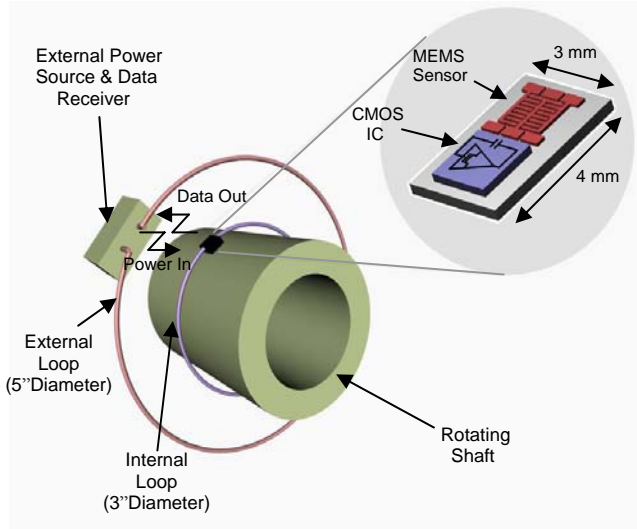


Figure 1. Stand-alone Microsystem Architecture

MEMS Strain Sensor

Figure 2 shows a simplified schematic of a capacitive MEMS strain sensor employed in the prototype system. The device consists of three amplifying buckled beams, critical for improving device sensitivity, with comb fingers positioned at the structural center. An externally applied

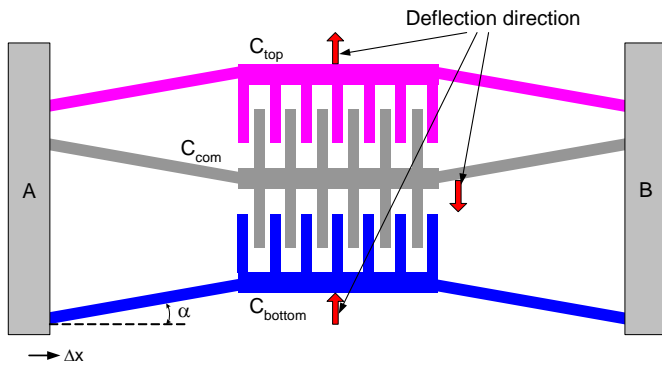


Figure 2. Capacitive Strain Sensor

strain introduces a small lateral displacement, Δx , which will result in an enhanced beams deflection along the vertical axis, upward for the C_{top} and C_{bottom} beams and downward for the center beam, C_{com} . The C_{top} and C_{bottom} electrodes thus form a set of linear differential capacitors (C_s^+ and C_s^-) with respect to the C_{com} electrode, serving as a common reference electrode as shown in the figure. The device sensitivity can be optimized by carefully selecting parameters such as buckling angle (α), finger numbers and thickness, and gap size. Optimized sensors exhibit a buckling angle of approximately 6° , a structural thickness of $20 \mu\text{m}$, a minimum air gap size of $3.6 \mu\text{m}$, and a lateral gauge length of 1 mm with 37 sets of center-positioned

fingers. The sensors have been fabricated by using DRIE on SOI substrates followed by releasing to free the microstructures [4]. Four fabricated sensors connected in parallel shown in Figure 3 achieve a nominal capacitance value of 0.44 pF with a differential sensitivity of 26.5 aF per $0.1 \mu\text{e}$, corresponding to a displacement of 1 \AA . Mechanical thermal noise, commonly referred to as Brownian motion, for the sensor is estimated several orders of magnitude lower than the minimum detectable

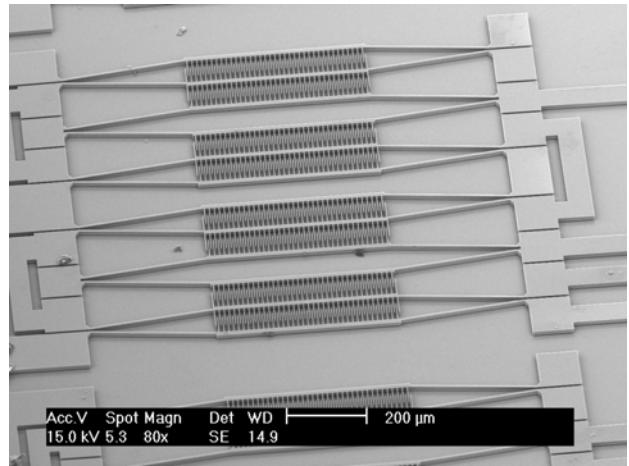


Figure 3. SEM of Fabricated Strain Sensors

signal requirement when operated in air. Therefore, low-noise sensing electronics are critical to interface with the sensor and achieve the overall stringent system performance requirements.

Low-Noise Interface Electronics

Capacitive sensor interface architectures employing switched-capacitor amplifiers typically exhibit an increased noise contribution due to aliasing of the high frequency amplifier thermal noise into the signal band [9-11]. Continuous time synchronous detection architecture, however, is attractive due to the amplifier low noise performance [12, 13] and is therefore employed in the prototype system, as shown in Figure 4.

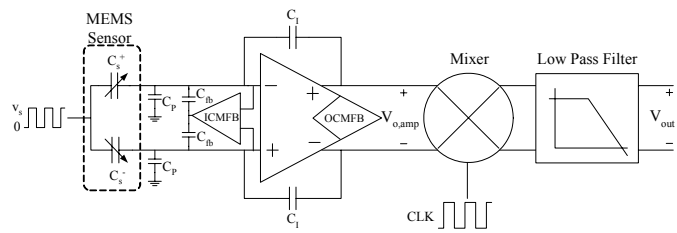


Figure 4. Electronic Strain Sensing Architecture

gain stage and the output buffers for achieving a large output signal swing. The entire sensing electronics consume 1.5 mA of DC current from a 2.8 V supply.

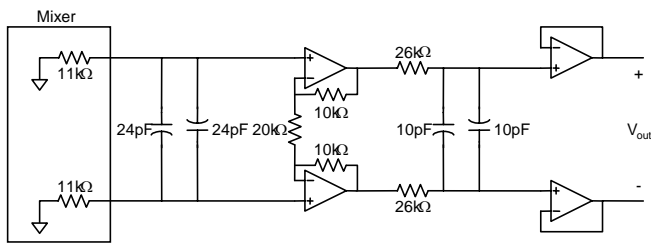


Figure 7. Low Pass Filter Architecture

Remote RF Powering System

Figure 8 shows the prototype remote RF powering system architecture.

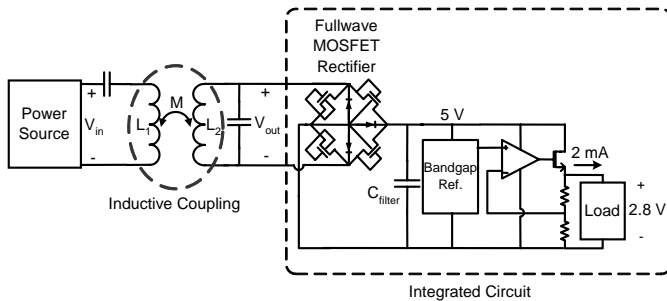


Figure 8. Remote RF Powering System Architecture

An external coil loop, L_1 , is driven by an RF power source and transfers the energy into a tuned internal coil loop, L_2 , through the coupling magnetic field, thus developing a sinusoidal output voltage, v_{out} , which is further rectified by a CMOS full-wave rectifier to provide a 5 V DC voltage. This 5V-supply, however, exhibits a strong ripple and is then further regulated by a CMOS regulator to output a stable 2.8 V DC supply with a 2 mA current driving capability. The voltage gain across the coupled loop inductors is a strong function of coil geometry, shaft material, and operating frequency [14]. Figure 9 presents the measured voltage gain versus operating frequency for various turn numbers of the internal loop based on the system configuration illustrated in Figure 1, employing an one-turn external coil loop. The measurement results indicate that a maximum voltage gain can be obtained with a properly tuned 3-turn internal coil loop operating at 50 MHz. A four-turn design results in an inferior performance due to an excessive iron shaft loss, which is not shown in the figure. An RF signal with an amplitude of 4 V at 50 MHz is thus required to achieve a DC voltage output of 2.8 V with 2 mA current driving capability, corresponding

to a power conversion efficiency of 11%. An improved efficiency is expected with an optimized transmitter power source design.

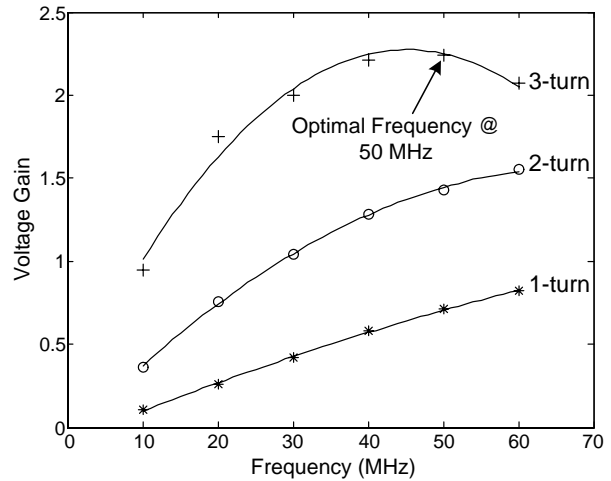


Figure 9. Voltage Gain vs Frequency with Various Internal Loop Turns

Measurement Results

The sensing and remote RF powering electronics are fabricated in a 1.5 μm CMOS process. Figure 10 shows the chip photo occupying an area of 2.2 mm x 2.2 mm.

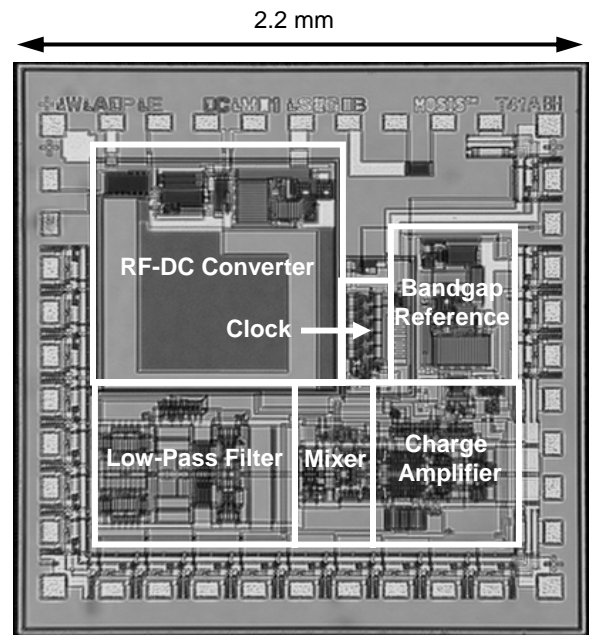


Figure 10. Electronics Die Photo

The MEMS sensor chip is first wire bonded to the sensing electronics to form the prototype system as shown in Figure 11. The sensor chip is then subjected to a three-point strain testing process for system characterization.

Figure 12 shows the measured output voltage versus an applied input strain when the sensing electronics are powered by a 2.8V battery, indicating that the prototype system can achieve a maximum input signal of 1000 $\mu\epsilon$, corresponding to an output voltage of 420 mV, with a linearity of 1.5% of full scale.

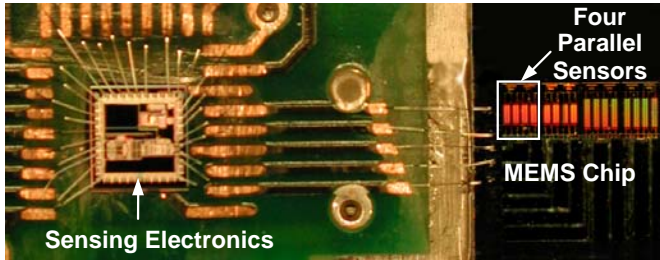


Figure 11. Prototype System Testing Board

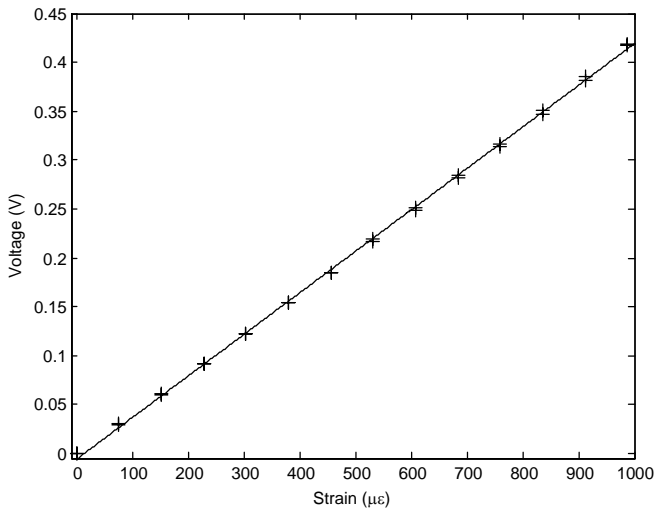


Figure 12. Output Voltage vs Input Strain

Figure 13 presents the measured output noise spectral density, demonstrating that the microsystem achieves a low noise level of $375 \text{ nV}/\sqrt{\text{Hz}}$, which is equivalent to a minimum detectable signal of $37.5 \mu\text{V}$ over a 10 KHz bandwidth, thus an 81 dB dynamic range. Considering the mixer conversion gain and noise from the mixer and low pass filter, the predicted noise performance is within 1 dB of the measurement results. A further reduced electronic noise floor is expected with improved CMOS technologies. The low frequency tone and $1/f$ noise are contributed by the measurement equipment.

The remote RF powering system characterization setup is shown in Figure 14. The 5 V-rectified and 2.8 V-regulated waveforms are presented in Figure 15. The stable DC voltage of 2.8 V exhibits a ripple of 45 mV peak-to-peak, a 16 mV/V of line regulation, and a 8mV/mA of load regulation.

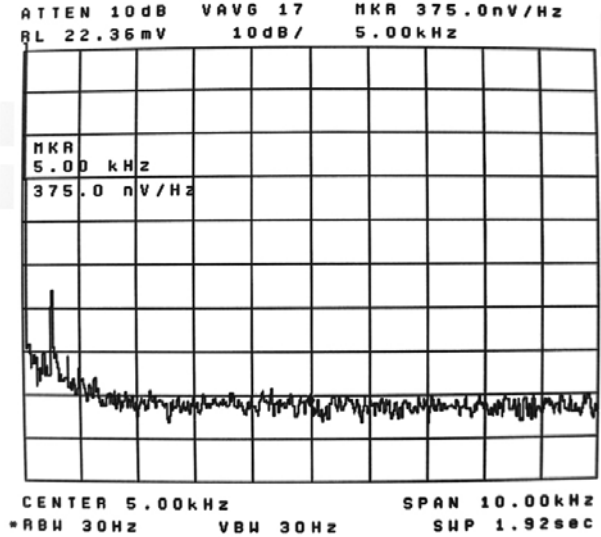


Figure 13. Output Noise Spectral Density

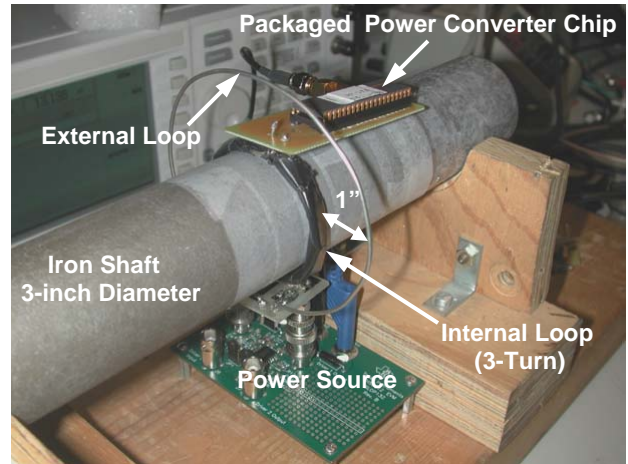


Figure 14. Remote RF Powering System Test Setup

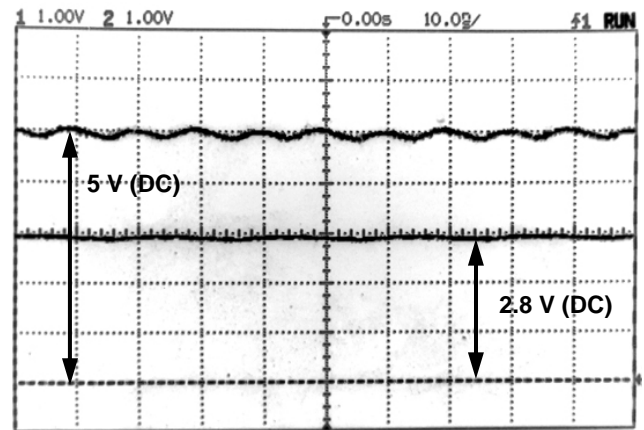


Figure 15. 5 V and 2.8 V DC Waveforms

The sensing electronics supplied by the remote RF powering system achieves a noise floor of $380 \text{ nV}/\sqrt{\text{Hz}}$, compared to the performance obtained by using a battery.

Conclusion

A high-performance strain sensing microsystem with a remote RF powering capability has been demonstrated. A MEMS capacitive strain sensor with amplifying buckled beams improves the device sensitivity. A low noise continuous time synchronous detection circuit is interfaced with the sensor to achieve an overall stringent system performance requirement. A stable remote RF powering architecture provides a DC supply voltage of 2.8 V with a 2 mA current driving capability, sufficient to power the microsystem. The prototype design demonstrates a strain sensing resolution of $0.09 \mu\text{e}$ over a 10 kHz bandwidth with 81 dB dynamic range, corresponding to a minimum detectable displacement of 0.9 \AA .

Acknowledgement

This work was supported by U.S. Army Research Office (ARO) under contract # DAAD19-02-1-0198.

References

- [1] M. L. Nagy, C. Apanius, and J. W. Siekkinen, "A User Friendly, High-Sensitivity Strain Gauge," *Sensors*, Vol. 18, pp. 20 – 27, June 2001.
- [2] M. Hrovat, D. Belavic, Z. Samardzija, and J. Holc, "An investigation of thick-film resistor, fired at different temperatures, for strain sensors," *International Spring Seminar on Electronics Technology*, pp.32-36, May 2001.
- [3] K. E. Wojciechowski, B. E. Boser, and A. P. Pisano, "A MEMS resonant strain sensor operated in air," *The Seventeenth Annual International Conference on Micro Electro Mechanical Systems (IEEE-MEMS)*, 2004, pp. 841-845.
- [4] J. Guo, H. I. Kuo, D. J. Young, and W. H. Ko, "Buckled beam linear output capacitive strain sensor", *Solid State Sensor, Actuator and Microsystems Workshop*, 2004.
- [5] L. Que, M.-H. Li, L. L. Chu, and Y. B. Gianchandani, "Measurements of material properties using differential capacitive strain sensors," *Journal of Microelectromechanical Systems*, Vol. 11, pp. 489-498, October 2002.
- [6] W. H. Ko, J. Hyncek, and J. Homa, "Single Frequency RF Powered ECG Telemetry System," *IEEE Transactions on Biomedical Engineering*, Vol. BME-26, No. 2, February 1979, pp. 105-109.
- [7] J. A. Von Arx, and K. Najafi, "A wireless single-chip telemetry powered neural stimulation system," *IEEE Int. Solid State Circuits Conf. (ISSCC) Dig. Tech. Papers*, 1999, pp. 214-215.
- [8] W. Liu and M. S. Humayun, "Retinal Prosthesis," *IEEE Int. Solid State Circuits Conf. (ISSCC) Dig. Tech. Papers*, 2004, pp. 218-219.
- [9] M. Lemkin and B. E. Boser, "A three-axis micromachined accelerometer with a CMOS position-sense interface and digital offset-trim electronics," *IEEE Journal of Solid-State Circuits*, Vol. 34, pp. 456-468, April 1999.
- [10] C. Junseok, H. Kulah, and K. Najafi, "An in-plane high-sensitivity, low-noise micro-g silicon accelerometer," *The Sixteenth Annual International Conference on Micro Electro Mechanical Systems (IEEE-MEMS)*, 2003, pp. 466-469.
- [11] N. Yazdi and K. Najafi, "An interface IC for a capacitive silicon μg accelerometer," *IEEE Int. Solid State Circuits Conf. (ISSCC) Dig. Tech. Papers*, 1999, pp. 132-133.
- [12] M. Tavakoli and R. Sarpeshkar, "An offset-cancelling low-noise lock-in architecture for capacitive sensing," *IEEE Journal of Solid-State Circuits*, Vol. 38, pp. 244–253, Feb. 2003.
- [13] J. Wu, G. K. Fedder, and R. Carley, "A low-noise low-offset chopper-stabilized capacitive-readout amplifier for CMOS MEMS accelerometers," *IEEE Int. Solid State Circuits Conf. (ISSCC) Dig. Tech. Papers*, 2002, pp. 428–429.
- [14] W. H. Ko, S. P. Liang, and C. D. F. Fung, "Design of Radio-Frequency Powered Coils for Implant Instruments," *Med. Biol. Eng. & Comput.*, Vol. 15, pp. 634-640, 1977.